Peptides 72 (2015) 164–174

Contents lists available at ScienceDirect

Peptides

journal homepage: www.elsevier.com/locate/peptides

Structure–activity relationship of mastoparan analogs: Effects of the number and positioning of Lys residues on secondary structure, interaction with membrane-mimetic systems and biological activity

Bibiana Monson de Souza[a,f], Marcia Perez dos Santos Cabrera[b], Paulo Cesar Gomes[c,f], Nathalia Baptista Dias[a,f], Rodrigo Guerino Stabeli[d], Natalia Bueno Leite[e], João Ruggiero Neto[e], Mario Sergio Palma[a,f,*]

[a] Institute of Biosciences, Department of Biology, Center for the Study of Social Insects, UNESP—Univ. Estadual Paulista, Campus of Rio Claro, Rio Claro, SP, Brazil
[b] Department of Chemistry and Environmental Sciences, IBILCE, UNESP—Univ. Estadual Paulista, Campus of São José do Rio Preto, São José do Rio Preto, SP, Brazil
[c] Department of Clinical Analysis, Proteomic Center, Faculty of Pharmaceutical Sciences, UNESP—Univ. Estadual Paulista, Campus of Araraquara, Araraquara, SP, Brazil
[d] Fundação Oswaldo Cruz, Ministério da Saúde, VPPLR, FIOCRUZ Rio de Janeiro, Rio de Janeiro, SP, Brazil
[e] Department of Physics, IBILCE, UNESP—Univ. Estadual Paulista, Campus of São José do Rio Preto, São José do Rio Preto, SP, Brazil
[f] Instituto Nacional de Ciência e Tecnologia (INCT) em Imunologia (iii), Salvador, BA, Brazil

ARTICLE INFO

Article history:
Received 3 March 2015
Received in revised form 16 April 2015
Accepted 19 April 2015
Available online 2 May 2015

Keywords:
Mastoparan
Wasp venom
Structure–activity relationship
Antimicrobial activity
Peptide synthesis

ABSTRACT

In this study, a series of mastoparan analogs were engineered based on the strategies of Ala and Lys scanning in relation to the sequences of classical mastoparans. Ten analog mastoparans, presenting from zero to six Lys residues in their sequences were synthesized and assayed for some typical biological activities for this group of peptide: mast cell degranulation, hemolysis, and antibiosis. In relation to mast cell degranulation, the apparent structural requirement to optimize this activity was the existence of one or two Lys residues at positions 8 and/or 9. In relation to hemolysis, one structural feature that strongly correlated with the potency of this activity was the number of amino acid residues from the C-terminus of each peptide continuously embedded into the zwitterionic membrane of erythrocytes-mimicking liposomes, probably due to the contribution of this structural feature to the membrane perturbation. The antibiotic activity of mastoparan analogs was directly dependent on the apparent extension of their hydrophilic surface, i.e., their molecules must have from four to six Lys residues between positions 4 and 11 of the peptide chain to achieve activities comparable to or higher than the reference antibiotic compounds. The optimization of the antibacterial activity of the mastoparans must consider Lys residues at the positions 4, 5, 7, 8, 9, and 11 of the tetradecapeptide chain, with the other positions occupied by hydrophobic residues, and with the C-terminal residue in the amidated form. These requirements resulted in highly active AMPs with greatly reduced (or no) hemolytic and mast cell degranulating activities.

Introduction

The search for new antibiotic substances found an almost inexhaustible source of potential therapeutic agents amongst antimicrobial peptides (AMPs), with sources including insect venoms. Nevertheless, the hidden promise turned into challenging holdbacks, such as difficulties and costs of synthesis of longer peptide sequences, narrower range of action, sensitivity of the short peptide chains to the physiological levels of salts, low toxicity for the host, and suitability of pharmacokinetic properties [13,14,18,38,42]. In the venom of wasps, mastoparan peptides represent good examples of antimicrobial peptides that have been intensively investigated [4,11,15,39–41]. Mastoparans are polycationic AMPs with 14 amino acid residues amidated at the C-terminus, with broad action against Gram-positive and Gram-negative bacteria and yeasts [4,27].

* Corresponding author at: Center for the Study of Social Insects/Department of Biology, IBRC-UNESP, Avenue 24A, 1515, Bela Vista, Rio Claro 13506 900, SP, Brazil. Tel.: +55 19 35264163; fax: +55 19 35348523.
E-mail address: mspalma@rc.unesp.br (M.S. Palma).

http://dx.doi.org/10.1016/j.peptides.2015.04.021
0196-9781/

Typically, mastoparans present three Lys residues at positions 4/5 and/or 11/12 [5,26,27,40]. One interesting exception is the peptide EMP-AF, in which Lys residues are at positions 5, 9 and 12 [7]. Hilpert et al. [18], working with a complete substitution library of a dodecapeptide derived from bactenecin, showed that certain positions are more sensitive to substitutions than others and that the introduction of certain amino acid residues, particularly charged ones, can generate peptides with increased antimicrobial activity. Kim and Cha [19], using model AMPs composed only of Leu and Lys residues, concluded that these peptides display different cationic distributions and that the dispersion of these amino acid residues on the hydrophilic surface is a factor that contributes to antimicrobial activity.

It was reported that the antimicrobial activities of mastoparan peptides bearing positive charges at the positions 4/5 and/or 11 to 13 were very active, while peptides presenting positive charges located in the middle of the peptide chain resulted in reduced activity [5,6,8,9]. It was suggested that the positioning of the Lys residues at those strategic sites would flank and maintain a stable helical segment, resulting in a more homogeneous hydrophobic surface in an amphipathic structure, which in turn contributes to the maximal lytic efficiency of the mastoparans. At the same time, Leite et al. [22] demonstrated the interplay between net charge and mean hydrophobicity, working with similar mastoparan peptides. These studies lead us to further investigate the role of the number and positioning of Lys residues along the peptide chain, taking into consideration their contribution to the following: (i) the number of amino acid residues of the hydrophilic and hydrophobic surfaces for the mean hydrophobicity per residue; (ii) the positioning of the peptide in relation to a model bilayer surface; (iii) the effects of these variables on the classical biological activities of mastoparans.

In this study, a series of novel peptides were engineered, considering the number and the positioning of Lys residues, with the sequences of known mastoparan peptides as a reference. Attempts were also made to optimize the antimicrobial activity while reducing the hemolytic activity and maintaining/reducing mast cell degranulation. The effects of two different strategies of residue replacement were investigated: (i) the individual replacement of Lys residues by Ala, one by one, in a type of Ala scan; and (ii) the replacement of Leu or Ala residues by Lys, in a type of Lys scan.

Materials and methods

Peptide synthesis and purification

The peptides were prepared by step-wise manual solid-phase synthesis using N-9-fluorophenylmethoxy-carbonyl (Fmoc) chemistry with Novasyn TGS resin (NOVABIOCHEM, Germany). Side-chain protective groups included *N*-β-trityl for asparagine and *t*-butoxycarbonyl for lysine. Cleavage of the peptide-resin complexes was performed by treatment with trifluoroacetic acid/1,2-ethanedithiol/anisole/phenol/water (82.5:2.5:5:5:5 by volume), using 10 mL/g of complex at room temperature for 2 h. After filtering to remove the resin, anhydrous diethyl ether (SIGMA, USA) at 4 °C was added to the soluble material, causing precipitation of the crude peptide, which was collected as a pellet by centrifugation at 1000 × *g* for 15 min at room temperature. The crude peptides were suspended in water and chromatographed under RP-HPLC using a semi-preparative column (SHISEIDO, Japan; C18, 250 × 10 mm, 5 μm) at a flow rate of 2 mL/min in the following isocratic conditions with acetonitrile in water (containing 0.1%(v/v) trifluoroacetic acid): 48% (v/v) for MK578, 47% (v/v) for MK89, 50% (v/v) for MK9, 50% (v/v) for MK5, 55% (v/v) for MK0, 37% (v/v) for MK4589, 39% (v/v) for MK5789, 35% (v/v) for MK58911, 33% (v/v) for MK45789, and 30% (v/v) for MK4578911. The elution was monitored at 214 nm using a UV-DAD detector (SHIMADZU, Kyoto, Japan; mod. SPD-M10A), and each fraction eluted was manually collected into 15 mL glass vials. The purified synthetic mastoparan analogs were dried under vacuum during 18 h at 4 °C, and then their weight were determined in a analytical balance.

The homogeneity and correct sequence of the synthetic peptides were assessed using a gas-phase sequencer PPSQ-21A (SHIMADZU, Japan) based on automated Edman degradation chemistry and ESI–MS analysis.

Liposomes preparation

Phospholipids supplied by Sigma-Aldrich Co. (St. Louis, MO) were dissolved in chloroform, and films were prepared using solutions of 100% egg L-α-phosphatidylcholine (PC) or 70% PC: 30% egg L-α-phosphatidyl-DL-glycerol (PCPG) by evaporating the solvent to dryness under N_2 flux. Small unilamellar vesicles (SUVs) were prepared by hydration of the phospholipid films with 5 mM Tris/H_3BO_3 buffer pH 8.0, containing 0.5 mM EDTA and 150 mM NaF, followed by sonication with a tip sonicator for 50 min under refrigeration by water bath and N_2 flux. Then, the preparation was subjected to 11 times extrusion through two stacked 50 nm pore size polycarbonate membranes (Nuclepore Track-etch Membrane, Whatman, USA), using an Avanti mini-extruder. Large unilamellar vesicles (LUVs) were prepared by hydration of the films with bi-distilled water at room temperature, followed by 6 times extrusion through 400 nm pore size polycarbonate membranes (Nuclepore Track-etch Membrane, Whatman) and then 11 times extrusion through two stacked 100 nm pore size membranes. Both types of vesicles were prepared to give approximately 10 mM lipids concentration; they were kept under refrigeration, protected from light and used on the day of preparation. The sizes of liposomes were confirmed by measurements of dynamic light scattering (DLS) using a Nano Zetasizer ZS90 (Malvern Instruments, Worcestershire, U.K.).

Secondary structure evaluation through circular dichroism (CD)

To evaluate the conformational changes of the peptides induced by membrane-mimetic environments, CD spectra were acquired at 20 μM peptide concentration in 2,2,2-trifluoroethanol (TFE)/bi-distilled water (40% v/v), in 8 mM sodium dodecyl sulfate solution (SDS), in 100 μM PC and 100 μM PCPG liposomes (SUVs). These spectra were compared with the spectra obtained in water and in Tris/H_3BO_3 buffer containing 150 mM NaF. CD spectra were recorded from 190 or 200 to 260 nm with a Jasco-710 spectropolarimeter (JASCO International Co. Ltd., Tokyo, Japan), which was routinely calibrated at 209 nm using D-pantolactone solution [20]. Spectra were acquired at 25 °C using a 0.5 cm path length cell and averaged over eight or nine scans at a scan speed of 20 nm/min, bandwidth of 1.0 nm, 0.5 s response and 0.1 nm resolution. Following baseline correction, the observed ellipticity, θ (mdeg), was converted to mean residue ellipticity, $[\Theta]$ (deg/cm^2/dmol), using the following relationship:

$$[\theta] = \frac{100\theta}{(lcn)},$$

where l is the path length in centimeters, c is the peptide millimolar concentration, and n is the number of peptide bonds. Assuming a two-state model, the observed mean residue ellipticity at 222 nm ($[\Theta]^{obs}{}_{222}$) was converted into the α-helix fraction (f_H) using the method proposed by Rohl and Baldwin [24,31].

Determination of the positioning of peptides in proteoliposomes by mass spectrometry

To access the positioning of the peptide backbone in relation to the surface of model membranes, electrospray ionization mass spectrometry (ESI-MS) was used to analyze the hydrogen/deuterium (H/D) exchange properties of peptides in D_2O solution or incorporated into LUVs (proteoliposomes) diluted with D_2O. After quenching deuteration by the addition of formic acid, the H/D exchange was directly analyzed by ESI–MS. The deuterated peptide ions were analyzed under collision induced dissociation (CID) mass spectrometry, which permitted the location of deuterons at the amide sites along the peptide backbone. Intramolecular hydrogen scrambling was investigated both for free peptides in solution and for their supramolecular structures as proteoliposomes, as described elsewhere [6,34].

Experiments were performed on a triple-quadrupole mass spectrometer (Micromass, Altrincham, UK), mod. Quattro-II, equipped with a standard ESI source. During all experiments, the source temperature was maintained at 80 °C and the capillary voltage at 1.80 kV; a drying gas flow (nitrogen) of 210 L/h and a nebulizer gas flow of 15 L/h were used. The mass spectrometer was calibrated with intact horse heart myoglobin and its characteristic cone-voltage-induced fragments; the cone-to-skimmer lens voltage controlling the ion transfer to the mass analyzer was manually set to 120 V. Before beginning the H/D exchange measurements, LUVs were incubated at 30 °C for at least 30 min.

SUVs in the presence or absence of peptides were pre-incubated for times ranging from 1 to 60 min at room temperature before measuring H/D exchange. The suspensions of liposomes in the presence of peptides were prepared for H/D exchange monitoring as described above, except for replacing bidistilled water with 99% (v/v) D_2O (Cambridge Isotopes Laboratories, Inc.). The free peptide solution was prepared for H/D exchange by adding 5 μL of peptide solution (1.2 μg/μL) to either 22 μL bidistilled water or liposome suspension and adding 50 μL 99% (v/v) D_2O following the liposome pre-incubation. The H/D exchange was allowed to proceed for 30 s and then quenched by adjusting the pH to 2.5 by the addition of 1 μL of 99% formic acid, followed by cooling to 0 °C. The solution of free peptides or the liposomes/peptide suspension was introduced into the mass spectrometer at a flow of 4 μL/min with a microperfusion pump (KD Scientific). Spectra were continuously acquired over 3 min by direct injection of the samples into the ionization source system. Each H/D exchange reaction was performed three times for each condition, and the tandem mass spectra were individually acquired for each replicate experiment. The mass-to-charge values of all ions of interest from each spectrum were used to calculate the rate values, with their respective standard deviations, and for the calculation of deuterium incorporation into the peptide. ESI spectra were acquired in continuous acquisition mode, scanning from m/z 200–2500, with a scan time of 7 s. Typical conditions used to perform the CID MS experiments were as follows: argon as the collision gas; capillary voltage of 1.78 kV, cone voltage of 120 V, collision energy of 135 eV, collision gas pressure of 4.10^{-4} mBar and desolvation gas temperature of 80 °C. In these experiments, the first quadrupole (Q1) was used to select precursor ions, which were fragmented in the hexapole (Q2) collision cell, generating product ions for subsequent mass analysis by the last quadrupole mass analyzer (Q3). Data acquisition was performed in continuous mode, scanning from m/z 40 to the m/z value of the monoprotonated form of the peptide $[M+H]^+$, with a scan time of 5 s, and monitored using the MassLynx software. Peptide sequences were manually assigned from ESI–MS/MS product ion mass spectra. Mass spectrometric measurements were begun as quickly as possible (the dead time was approximately 90 s), and analyses were performed in MS and MS/MS modes. Each H/D exchange reaction was performed five times for each condition, and the tandem mass spectra were individually acquired for each replicate experiment. The mass-to-charge values of all fragment-ions of interest from each spectrum were used to calculate the rate values with the respective standard deviations and to calculate deuterium incorporation into the peptide.

Biological activities

Mast cell degranulation

Mast cell degranulation was determined by measuring the release of β-D-glucosaminidase, which co-localizes with histamine. Mast cells were obtained by peritoneal washing of Wistar rats with a solution containing 0.877 g NaCl, 0.028 g KCl, 0.043 g NaH_2PO_4, 0.048 g KH_2PO_4, 0.10 g glucose, 0.10 g BSA, 90 mL 2 M $CaCl_2$ solution, and 50 μL Liquemine (heparin, Roche) in 100 mL water. The mast cells were incubated in the presence of various peptide concentrations for 15 min at 37 °C. Then, 50 μL of the mast cell suspensions was added to 50 μL of the substrate, which consisted of 3.4 mg of *p*-nitrophenyl-*n*-acetyl-β-D-glucosaminidine (Sigma-Aldrich, St. Louis, MO) dissolved in 10 mL of 200 mM sodium citrate solution at pH 4.5 and incubated for 6 h at 37 °C. The reaction was interrupted by the addition of 150 μL of 0.2 M Tris solution; after centrifugation, the supernatants were sampled for the b-D-glucosaminidase assay, and the absorbance of the colored product was assessed at 405 nm in a microtiter plate reader (Biotrack, Amersham Bioscience). The values were expressed as the mean percentage of total b-D-glucosaminidase activity from five experiments with rat mast cell suspensions, in relation to mast cells lysed by the addition of 0.1% (v/v) Triton X-100 (considered as 100% reference).

Hemolysis

Five hundred microliters of washed rat red blood cells (WRRBC) was suspended in 50 mL of physiological saline solution (0.9% (w/v) NaCl). Ninety microliters of this suspension was incubated with 10 mL of peptide solution at different concentrations at 37 °C for 2 h. The samples were then centrifuged, and the absorbance of the supernatants was measured at 540 nm. The absorbance measured from lysed WRRBC in the presence of 1% (v/v) Triton X-100 was considered to be 100%. The results are expressed as the mean ± S.D. of five experiments.

Antimicrobial activity

The minimal inhibitory concentrations (MIC) of the peptides were determined based on methods described by Meletiadis et al. [25]. The following microorganisms were used: *Escherichia coli* (CCT 1457), *E. coli* (ATCC 11775), *E. coli* (ATCC 25922), *Pseudomonas aeruginosa* (ATCC15442), *P. aeruginosa* (ATCC13388), *Salmonella choleraesuis* (ATCC10708), *Salmonella typhimurium* (ATCC14028), *Staphylococcus aureus* (CCT 2580), *S. aureus* (CCT 6538), *S. aureus* (ATCC 25923), *Staphylococcus epidermides* (ATCC12228), *Staphylococcus pneumoniae* (ATCC11733), *Staphylococcus mutans* (AU159), *Bacillus cereus* (ATCC11778), *Bacillus thuringiensis* (ATCC10792), *Enterococcus faucium* (CCT5079), *Enterococcus hirae* (ATCC10541), *Rhodococcus equi* (ATCC25729), and *Micrococcus luteus* (ATCC4698). The experiment was performed in 96-well plates. Bacterial cells were suspended in sterile culture medium; the inoculum size was 1×10^4 cells m/L in Müller–Hinton broth (DIFCO), confirmed by the use of the McFarland scale. From this culture, 50 mL was spread onto a micro-plate previously containing 50 mL of Müller–Hinton broth, resulting in a final cell density of 1.5×10^3 cell/mL. Cells were incubated at 37 °C for 18 h in the presence of 100 mL of each peptide solution, in a concentration range from 0.8 to 50 mg/mL. After incubation, 10 mL of a triphenyltetrazolium chloride (TTC) (MALLINCKRODT) solution (final concentration 0.05%, w/v) was

added to each well plate. The plate was incubated at 37 °C for 2 h. Live colonies reduce TTC to a dark red color, while colonies with reduced respiratory function are unable to perform this reduction and instead remain unchanged in color. Thus, the results were expressed as the MIC that inhibits all colony-forming units. Chloramphenicol (Sigma-Aldrich) was used as a standard antibiotic, and wells containing only the culture medium were used as negative controls. The results are expressed as the mean of three experiments.

Results

Design of peptide sequences

To investigate the effect of the number and positioning of Lys residues on the secondary structure of the peptides, the interaction of each peptide with the bilayer surface, and the resulting biological activities, a set of ten tetradecapeptides, amidated at the C-terminus, were synthesized and purified; these peptides included from zero to six Lys residues, at positions from +1 to +7. Table 1 shows the sequences of these peptides, their respective net charges, and the values of mean hydrophobicity and hydrophobic moment, calculated according to the consensus scale of Eisenberg et al. [12]. The nomenclature used to identify the peptides considered their derivation from **M**astoparans and the presence of Lys (**K**) in the sequence; the numbers represents the positioning of each **K** residue. Thus, the peptide MK578 represents a **M**astoparan with **K** residues at positions **5**, **7**, and **8**, while MK0 represents a **M**astoparan with no **K** residue in the sequence.

Secondary structure evaluation

The secondary structures of the peptides were determined by CD spectroscopy in the presence of water and buffer, in membrane-mimetic environments, and in the presence of model membranes. Comparative spectra of peptides MK578, MK89 and MK4589 are shown in Fig. 1, while the spectra of remaining peptides and the respective values of mean residue molar ellipticity at 222 nm are shown in the supplementary information (Fig. S1). Peptides MK89 and MK4589 present higher intensity spectra at 222 nm than MK578 in the presence of 40% (v/v) TFE, in 8 mM SDS and in 100 μM PCPG vesicles, indicating that in these environments, higher helical content was induced. In the presence of 100 μM PC vesicles, peptide MK89, one of the analogues with higher hydrophobicity (Table 1), presents a spectrum compatible with the induction of α-helical structures, while the spectra of MK578 and MK4589 are typical of random coil structures, reflecting poor binding to the membrane-mimetic system.

In water, the CD spectra of the peptides show a negative band near 200 nm, indicating a random coil conformation, except for MK0, which has characteristics of β-turn structure, showing a negative band at approximately 220 nm and a positive band of much higher intensity at approximately 197 nm (Supplementary Fig. S1). In aqueous solution of 40% (v/v) TFE or in micellar SDS (8.0 mM), the spectra present two negative dichroic bands at 222 and 208 nm, which are characteristic of α-helical conformation for most peptides. Slight deviations from these values (219–221 and 205–209 nm) were found for MK578 and MK5. Important deviations were found for the most hydrophobic and the most hydrophilic peptides, MK0 and MK4578911, respectively (Supplementary Fig. S1). They show certain characteristics of helical peptides in the presence of 40% (v/v) TFE solution and certain characteristics of β-turn in the presence of 8 mM SDS, displaying negative bands, respectively, at 218 nm and 225 nm and positive bands at 195 nm. Zwitterionic liposomes were not able to induce

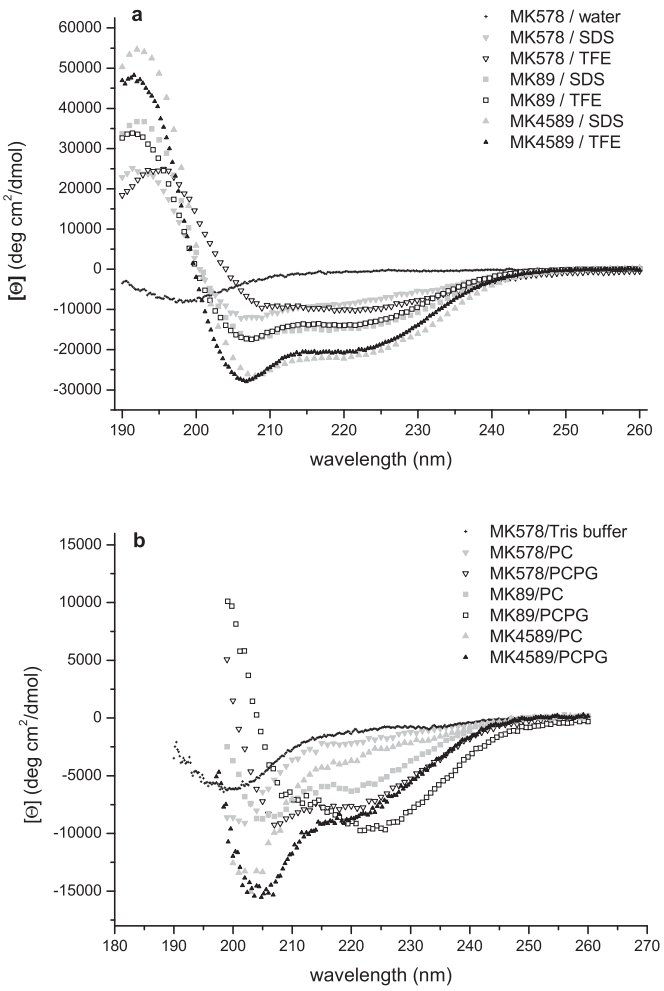

Fig. 1. CD spectra of peptides MK578, MK89 and MK4589 obtained at 20 μM and 25 °C. (a) MK578 in water, in 8 mM SDS and in 40% TFE solution; MK89 and MK4589 in 8 mM SDS and in 40% TFE solution. (b) MK578 in buffer, in zwitterionic PC SUVs at 100 μM and in anionic PCPG SUVs at 100 μM; MK89 and MK4589 in PC SUVs at 100 μM and in anionic PCPG SUVs at 100 μM. No smoothing has been applied.

conformational changes in MK578 and in the hydrophilic peptides (MK4589, MK5789, MK58911, MK45789, MK4578911), which show random coil conformations, but the analogues MK89, MK9 and MK5 present spectra characteristic of helical peptides. Additionally, in presence of vesicles, MK0 and MK4578911 present different secondary structures from the remaining analogues: in PC and in PCPG vesicles, MK0 shows characteristics of β-turn structures, while MK4578911 shows a random coil configuration (Supplementary Fig. S1). Anionic liposomes induced α-helical conformation in all other analogues. Values of mean residue molar ellipticity at 222 nm are shown in Supplementary Table S1 (electronic Supplementary information). Signs of possible peptide aggregation were found for MK578 in 40% (v/v) TFE, for MK89 and MK9 in PCPG, and for MK5 in PC and in PCPG, as indicated by the relationship between molar ellipticities at 222 and 208 nm, $[\Theta]_{222} > [\Theta]_{208}$ [3].

From the values of mean residue molar ellipticity at 222 nm, the α-helix fractions were calculated for all ten MK peptides (Table 2). MK4589 is the peptide with the highest ellipticity in 8 mM SDS and in 40% (v/v) TFE. Most of peptides in this study presented similar helical content in the presence of SDS or in TFE; only the peptides MK0, MK578, and MK4578911 presented low α-helix content under these conditions. Peptides MK578, MK4589, MK5789, MK58911, and MK4578911 (peptide analogs with net charge ≥+5)

Table 1
Sequences of engineered mastoparans with Lys residues shown in bold face, with respective values of net charge (Q) at physiological pH, mean hydrophobicity per residue $\langle H \rangle$ and hydrophobic moment of designed mastoparan analog peptides (μ).

Peptides	Sequences														Q[a]	$\langle H \rangle$[b]	μ[b]
MK578	I	N	W	L	**K**	A	**K**	**K**	V	A	G	M	I	$L\text{-}_{NH_2}$	+4	0.029	0.104
MK89	I	N	W	L	A	I	A	**K**	**K**	V	A	G	M	$L\text{-}_{NH_2}$	+3	0.126	0.185
MK9	I	N	W	L	A	I	A	A	**K**	V	A	G	M	$L\text{-}_{NH_2}$	+2	0.222	0.168
MK5	I	N	W	L	**K**	I	A	A	A	V	A	G	M	$L\text{-}_{NH_2}$	+2	0.222	0.163
MK0	I	N	W	L	A	I	A	A	A	V	A	G	M	$L\text{-}_{NH_2}$	+1	0.319	0.072
MK4589	I	N	W	**K**	**K**	I	A	**K**	**K**	V	A	G	M	$L\text{-}_{NH_2}$	+5	−0.087	0.279
MK5789	I	N	W	L	**K**	I	**K**	**K**	**K**	V	A	G	M	$L\text{-}_{NH_2}$	+5	−0.067	0.191
MK58911	I	N	W	L	**K**	I	A	**K**	**K**	V	**K**	G	M	$L\text{-}_{NH_2}$	+5	−0.067	0.242
MK45789	I	N	W	**K**	**K**	I	**K**	**K**	**K**	V	A	G	M	$L\text{-}_{NH_2}$	+6	−0.184	0.216
MK4578911	I	N	W	**K**	**K**	I	**K**	**K**	**K**	V	**K**	G	M	$L\text{-}_{NH_2}$	+7	−0.280	0.248

[a] Includes an extra charge due to the amidated C-terminus.
[b] Calculated according to Eisenberg et al. consensus scale [12].

Table 2
The α-helix fraction for the complete series of MK peptides, calculated according to a two-state model [31].

$f_{(H)}$	Water	TFE 40%	SDS 8 mM	PC	PCPG
MK578	Rc	0.31	0.25	rc	0.23
MK89	Rc	0.43	0.46	0.18	0.30
MK9	Rc	0.45	0.42	0.29	0.37
MK5	Rc	0.46	0.44	0.37	0.42
MK0	Bt	0.29	Bt	bt	bt
MK4589	Rc	0.65	0.69	rc	0.26
MK5789	Rc	0.58	0.42	rc	0.22
MK58911	Rc	0.60	0.51	rc	0.26
MK45789	Rc	0.54	0.51	rc	0.19
MK4578911	Rc	0.38	Bt	rc	rc

rc = Random coil; bt = β-turn-like structure.

showed selective interaction in relation to the anionic PCPG vesicles compared to the zwitterionic PC vesicles, presenting only random coil under this condition. The lower helical content of most peptides in anionic vesicles compared to SDS micelles may be due to insufficient charge neutralization by the PCPG vesicles.

Determination of the positioning of peptides in proteoliposomes by mass spectrometry

The interaction of peptides with vesicles was investigated using a homogeneous population of LUVs presenting a diameter of 130 ± 8 nm. The binding and positioning of the peptides in relation to the LUV surface was monitored by ESI–MS/MS through H/D exchange in proteoliposomes. H/D exchange mass spectrometry assays can show how the peptide backbone interacts with membranes [6,34]. In this technique, the site-specific locations of deuteron positions in the peptide–membrane-mimetic systems are determined, indicating which amino acid residues of the peptide chain are positioned in the inner core of the membrane and which ones are interacting with the outside medium [34]. In this study, all the peptides were analyzed in the presence of water, zwitterionic PC vesicles and anionic PCPG vesicles; peptide MK578 is used as an example in Fig. 2. To save printing space, only the mass spectra of MK578 are shown in the main text, while the spectra of the other peptides are presented as electronic supplemental information (Supplementary Figs. S2–S10).

Fig. 2A shows the CID spectra for studying the H/D exchange of MK578 in the presence of water, while Fig. 2B and C shows the CID spectra in the presence of PC and PCPG vesicles and D_2O, respectively. In the presence of water, the CID spectrum (Fig. 2A) shows a clear pattern of fragmentation, with easy interpretations of the MK578 sequence; the pattern of fragmentation of all peptides was characterized by the formation of a dipeptide at the N-terminus of each peptide. The CID spectrum in the absence of liposomes but in the presence of D_2O is not shown, as all the amino acid residues of the sequences became deuterated under this condition in all ten peptides assayed.

In the presence of PC vesicles, the backbones of residues Ile1, Ans2, Leu4, Lys5, Ala6, Lys8, Val9, and Ile13 were labeled with deuterium, identifying their position located outside the bilayer surface. In the presence of PCPG vesicles, the interaction was observed to be slightly shallower than in the presence of PC vesicles, because the backbones of nine residues were labeled (positioned outside the vesicle membrane): Ile1, Ans2, Leu4, Lys5, Ala6, Val9, Ala10, Gly11 and Ile13 (Fig. 2B and C). In both environments, the C-terminus was embedded in the inner core of the membrane (not deuterated), while the N-terminus was labeled with deuterium, indicating that this region does not access the interior of the membrane during the H/D exchange process.

Based on the data obtained from the CID MS spectra of the remaining peptides (Figs. S2–S10), the pattern of H/D exchange for each peptide was interpreted in the presence of water, as well in the presence of PC and PCPG vesicles; diagrams representing the interactions of the peptides with the surfaces of the PC and PCPG membranes are shown in Fig. 3. A common feature amongst these peptide interactions with both types of vesicles is that their N-termini residues/regions are exposed to the solvent medium, while their C-termini residues/regions are embedded in the bilayer environment. This observation is consistent with the charged nature of the N-terminal residues, as previously reported for other mastoparan peptides [34]. The amidation of the C-terminal residues of mastoparans was also reported to be an important structural feature in maintaining the helical secondary structure of these peptides [33].

Biological activities

The biological activities of all MK analogue peptides were investigated by assaying mast cell degranulation, hemolysis, and antimicrobial activities. Fig. 4 shows the results for rat peritoneal mast cell degranulation. Peptide HRII was used as the standard for mast cell degranulation [1,2]. Analogues MK89 and MK9 presented the highest degranulation activity, while all the other analogues presented greatly reduced degranulation activity.

The hemolytic activity on rat erythrocytes is shown in Fig. 5A and B. Peptides MK5, MK89, MK9, and MK58911 presented the highest hemolytic activity amongst all the MK analogs. Curiously, all the remaining peptides presented reduced hemolytic activities despite their large differences in net charge and hydrophobicity.

The antibiotic assays against Gram-positive and Gram-negative bacteria were performed for all ten MK analog peptides, and the results are summarized in Table 3. It may be observed that peptides MK4589, MK45789, and 4578911 were highly active against the Gram-negative bacteria, especially MK4589, which was more potent that the reference antibiotic, chloramphenicol.

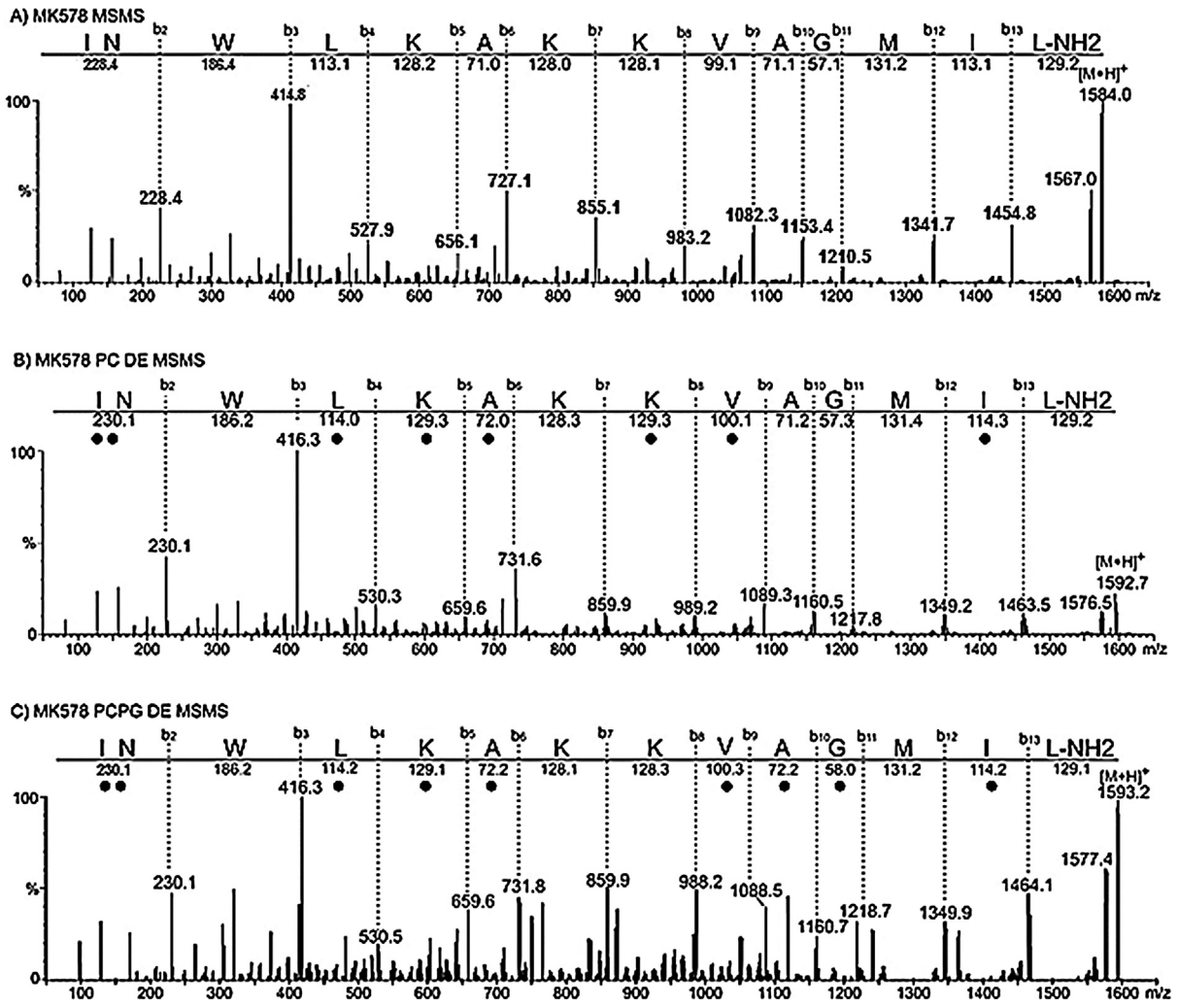

Fig. 2. CID MS spectra of MK578, acquired under continuous infusion of the peptide solution into the mass spectrometer. Each spectrum represents the combination of scans within 1 min of data acquisition: (A) peptide in water in the absence of D_2O (monoisotopic molecular ion at *m/z* 1584.0 as $[M+H]^+$); (B) peptide as proteoliposomes (LUVs) with PC in the presence of D_2O (monoisotopic molecular ion at *m/z* 1592.7 as $[M+H]^+$; and (C) peptide as proteoliposomes (LUVs) with PCPG in the presence of D_2O (monoisotopic molecular ion at *m/z* 1593.2 as $[M+H]^+$; The mass differences between the consecutive b_n ions and their correspondence to the deduced amino acid sequences are shown. The black dots (•) assigned over the symbols of certain amino acid residues correspond to the location of deuterons at specific amide hydrogens.

Table 3
Antibiotic activity of MK analog peptides against Gram-positive and Gram-negative bacteria, expressed as minimum inhibitory concentration (MIC).

	MIC (μg/mL)										
	MK578	MK89	MK9	MK5	MK0	MK4589	MK5789	MK58911	MK45789	MK4578911	Chloramphenicol
Gram-negative											
E. coli (CCT 1457)	31	4	250	31	>500	1	8	4	4	1	1
E. coli (ATCC 11775)	63	8	500	500	>500	4	31	16	4	16	4
E. coli (ATCC 25922)	23	4	250	125	>500	4	31	31	16	16	1
P. aeruginosa (ATCC15442)	125	16	500	31	>500	8	125	16	8	16	16
P. aeruginosa (ATCC13388)	250	63	500	500	>500	16	250	8	4	16	31
S. choleraesuis (ATCC10708)	500	16	500	500	>500	8	500	31	31	31	8
S. typhimurium (ATCC14028)	500	31	500	500	>500	2	31	8	4	8	8
Gram-positive											
S. aureus (CCT 2580)	43	4	4	1	>500	2	8	4	2	2	1
S. aureus (CCT 6538)	63	4	16	250	>500	1	31	8	4	63	16
S. aureus (ATCC 25923)	63	8	16	250	>500	2	2	4	2	2	8
S. epidermides (ATCC12228)	63	4	16	63	>500	1	4	2	1	1	16
S. pneumoniae (ATCC11733)	125	2	1	2	>500	1	2	1	1	1	8
S. mutans (AU159)	500	4	250	500	>500	2	4	8	4	16	16
B. cereus (ATCC11778)	16	16	125	125	>500	16	250	31	31	125	4
B. thuringiensis (ATCC10792)	125	8	125	125	>500	31	125	31	31	125	8
E. faucium (CCT5079)	250	8	250	500	>500	1	8	1	2	2	2
E. hirae (ATCC10541)	63	8	250	500	>500	8	31	16	31	63	2
R. equi (ATCC25729)	250	4	250	250	250	1	2	2	2	8	16
M. luteus (ATCC4698)	31	4	15.6	125	>500	1	4	2	1	1	16

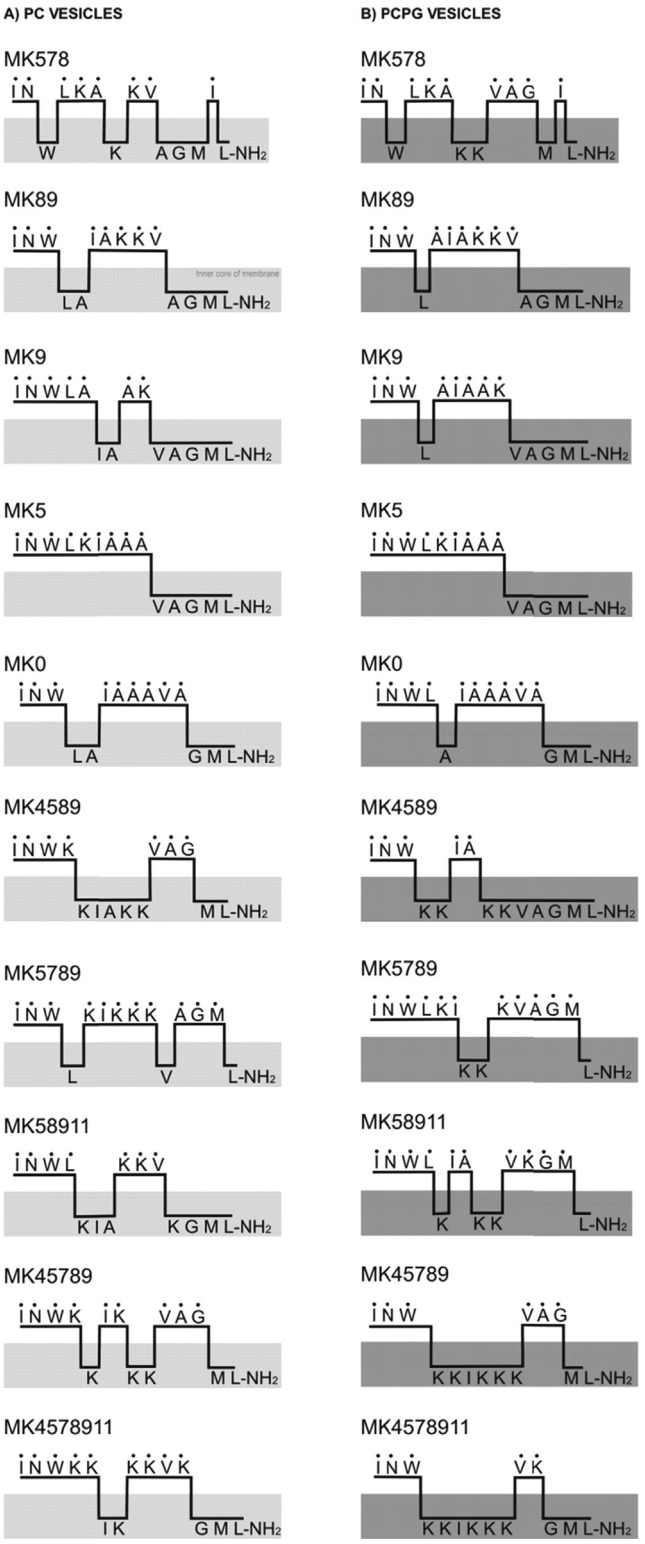

Fig. 3. Schematic representation of peptide/membrane interaction obtained from proteoliposome H/D exchange assay combined with ESI–MS/MS mass spectrometry for all mastoparan analogs of the MK series in the presence of PC (A) and PCPG (B) vesicles. The gray region represents the inner side of the membrane. The black dots (•) represent deuterium labeled sites. Thus, residues identified with a black dot are positioned outside the vesicle membrane, while residues embedded into the membrane lack the black dot in the grey region.

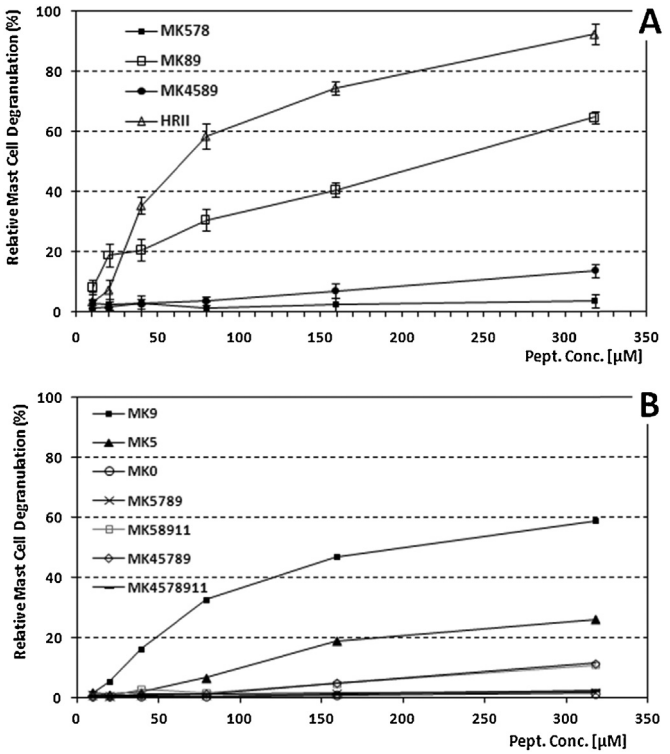

Fig. 4. Mast cell degranulation activity in rat peritoneal mast cells. The activity was determined by measuring the release of the granule marker, β-D-glucosaminidase, which co-localizes with histamine, and the values for β-D-glucosaminidase released in the medium were expressed as a percentage of total β-D-glucosaminidase. Values are mean ± S.D. ($n = 5$). (A) shows the profiles of activities of the standard peptide HR II and the mastoparan analogs MK89, MK578, and MK4589, while (B) shows the activities of the analogs MK0, MK5, MK9, MK5789, MK58911, MK45789, and MK4578911.

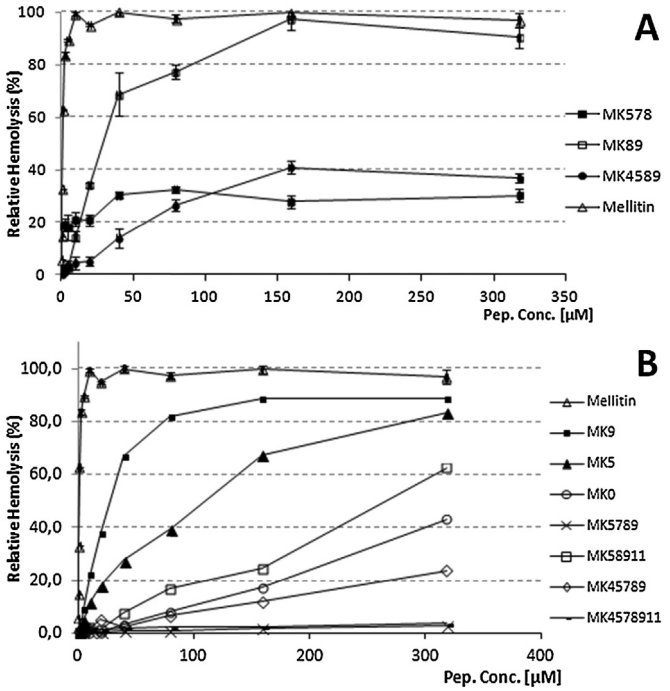

Fig. 5. Hemolytic activity in washed rat red blood cells (WRRBC). The absorbance measured at 540 nm from lysed WRRBC in the presence of 1% (v/v) Triton X-100 was considered as 100%. Values are mean ± S.D. ($n = 5$). (A) shows the activity profiles of mellitin (standard peptide) and the mastoparan analogs MK89, MK578, and MK4589, while (B) shows the activities of mellitin and the analogs MK0, MK5, MK9, MK5789, MK58911, MK45789, and MK4578911.

Meanwhile, the mastoparan analogs MK89, MK4589, MK45789, and MK4578911 were very active against the eleven different species of Gram-positive bacteria, especially peptide MK4589, which again was more active than the reference antibiotic compound chloramphenicol.

Discussion

Mastoparan peptides usually perform their roles in vertebrates both through the activation of mast cell exocytosis, delivering the granule contents to the media, especially histamine, and by perturbing erythrocyte membranes, leading to hemolysis [30]. Mast cell degranulation may occur by mastoparan binding to the extracellular receptor of G_α subunit of a trimeric G-protein controlling the exocytosis process, and in addition, some of these peptides can penetrate into mast cells and activate both the Ca^{2+}-independent and Ca^{2+}-dependent FcRI-mediated exocytosis pathways to enhance the potency of the inflammatory actions caused by the mastoparans as toxins [16,17,28,32,35]. Thus, mastoparan peptides seems to play their roles in mast cells through direct binding to specific receptors at the extracellular cell surface and/or at the level of endosomal receptors, which requires the recognition of a well-defined secondary structure of the ligand (mastoparan) by the receptors. It is not clear what structural and/or physicochemical factors regulate the ligand-receptor affinity for mastoparans.

Mastoparan peptides can also cause erythrocyte lysis, leading to hemolysis; apparently, the mastoparans interact with the zwitterionic membrane of these cells through the "carpet" mechanism, causing pore formation and structural perturbations that lead to cytolysis [29,34]. For this reason, mastoparans have been used as models for the development of AMPs [4,11,15,40,41]. A series of publications have reported the contributions of different physicochemical parameters to the optimization of the antimicrobial activity of mastoparans and/or the minimization of other parallel activities; however, there is no rational panel of factors explaining the interaction between mastoparans and animal and bacterial cell membranes. The mastoparan Polybia-MP I presented an anticancer effect (both in vitro and in vivo) against prostate tumor and leukemic cells but presented no effect against healthy cells [36]; the apparent selectivity for tumorigenic cells was attributed to the presence of phosphatidylserine in the outer leaflet of these cells, which is generally absent in healthy cells [37]. This explanation was latter corroborated, demonstrating that the high content of anionic lipids in the membranes increases the level of binding of the peptide to bilayers, favoring the anti-cancer effect of mastoparans [11]. It was also reported that mastoparans cause gradual cell leakage due to their accumulation on the membrane surface, inducing a transient interruption of its barrier properties and the leakage of cell contents. The membrane recovers its continuity inhomogeneously, creating a type of ply with peptides sandwiched between the juxtaposed faces of the membranes. Periodically, a peptide and lipid aggregate together, forming a lump with a high peptide-to-lipid ratio [10]. In relation to the actions of AMPs, a substitution library of a dodecapeptide derived from bactenecin was created, which demonstrated that certain positions in the peptide sequences are more sensitive to substitution than others and that the introduction of certain amino acid residues, particularly charged ones, can produce peptides with increased antimicrobial activity [18]. Using model AMPs composed only of Leu and Lys residues, Kim and Cha [19] synthesized a series of peptides presenting different cationic distributions, demonstrating that the dispersion of cationic amino acid residues on the hydrophilic surface is a factor that contributes to the antimicrobial activity. De Souza et al. [5] reported that the antimicrobial activities of mastoparan peptides bearing positive charges at the positions 4/5 and/or from 11 to 13 were highly active, while peptides presenting positive charges located in the middle of peptide chain exhibited reduced activity. It was suggested that the positioning of the Lys residues at those strategic sites was flanking and maintaining a stable helical segment, resulting in a more homogeneous hydrophobic surface in an amphipathic structure, contributing in turn to the maximal lytic efficiency of the mastoparans. At the same time, Leite et al. [22] demonstrated the interplay between net charge and mean hydrophobicity, working with similar mastoparan peptides. These studies stimulated the further investigation of the contributions of the number and positioning of Lys residues along the peptide chain; thus, a series of novel mastoparan analogs was engineered based on the rationale of reducing the number of hydrophobic residues in the hydrophilic face of the peptides molecule. This approach permitted investigation of the effects of the number and location of the residues of Lys in the peptide chain, as well as the influence of the net charge at physiological pH, mean hydrophobicity, and hydrophobic moment, on the biological activities of the mastoparan analogs (mast cell degranulation, hemolysis, and antimicrobial action).

Structural characterization of MK analogs

Typically, mastoparans present three Lys residues at positions 4/5 and/or 11/12 [4,5,26,27,39,40]; an interesting exception is the peptide EMP-AF, in which the Lys residues are at positions 5, 9 and 12 [7]. The series of mastoparan analogs synthesized resulted in peptides presenting from zero to six Lys residues, with net positive charges from +1 to +7, mean hydrophobicities from −0.280 to 0.319, and hydrophobic moments from 0.072 to 0.279 (Table 1).

The CD spectroscopy analysis revealed that all the peptides presented random coil as their secondary structure in the presence of water. Meanwhile, in the presence of 40% (v/v) TFE and 8 mM SDS, the peptide with no Lys residue in its sequence (MK0) has no α-helix in its secondary structure; all the other MK peptides presented from 42 to 69% α-helix in their secondary structures (Table 2). Regarding interaction with membrane mimetic-systems, the CD data in the presence of anionic PC vesicles showed that only the analogs MK89, MK9, and MK5 presented some fraction of α-helix in their secondary structure (from 18 to 37%). However, in the presence of zwitterionic PCPG vesicles, the peptides MK0 and MK4578911 (presenting zero and six Lys residues, respectively) presented only β-turn-like secondary structure, while the other MK analogs presented from 19 to 42% α-helix in their secondary structures (Table 2).

The helical wheel representation of the ten MK analogs is shown in Fig. 6, where it is possible to observe the increasing hydrophilic surface of the peptides as the number of Lys residues increases along their sequence. It is important to emphasize that this type of representation is purely hypothetical, as the whole secondary structures of all peptides are considered 100% helical. This supposition is not completely true, as the CD data (Table 2) reveal that only in the presence of 40% (v/v) TFE do all the peptides present some level of helicity (from 31 to 65%). The hydrophilic surfaces were initially considered to extend from the N-terminal residue (which becomes protonated at physiological pH) to the residue Asn 2; this surface contains five amino acid residues, three of them hydrophobic (in the peptide MK0). The introduction of Lys residues into this surface (at positions 5 or 9) contributed to making this surface more positive, as reflected in the decreasing mean hydrophobicity values and increasing hydrophobic moments (see Table 1). The replacements of certain hydrophobic residues at positions 7, 8, 9, and 11 resulted in a large increase in the hydrophilic surface (Fig. 4), with a consequent decrease in the mean hydrophobicity values per residue. Thus, the decreasing order of the hydrophilic surface for

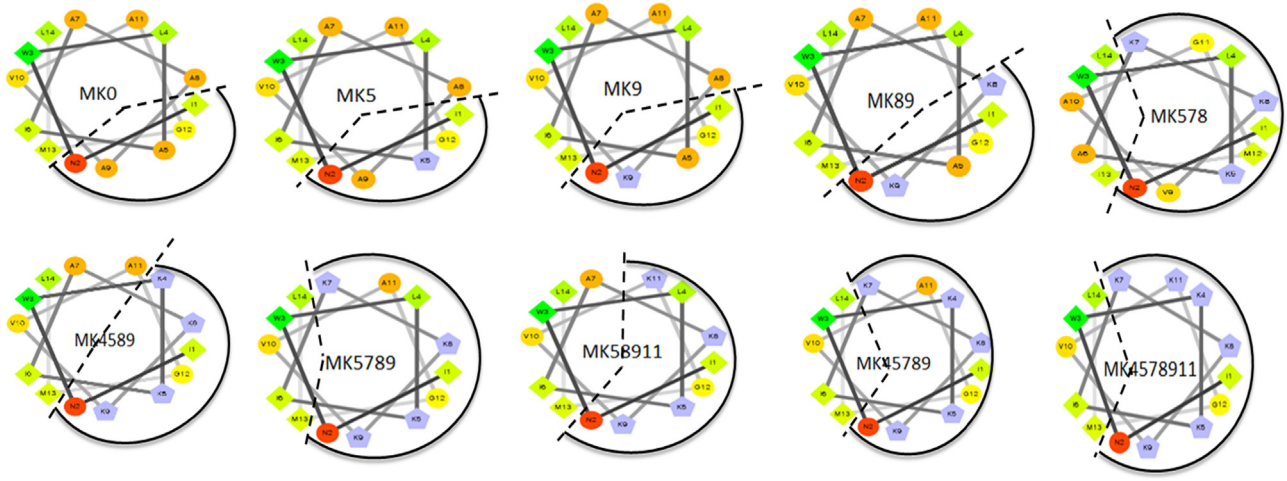

Fig. 6. Helical wheel representation of the ten mastoparan analogs of the MK series. The dashed lines delimiting the curved line represent the hydrophilic surface of each peptide.

the mastoparan MK analogs is as follows: MK4578911, MK45789, MK578 > MK58911, MK5789 > MK4589 > MK89 > MK0, MK5, MK9.

The interaction of mastoparan MK analogs with membrane-mimetic system

The H/D exchange experiments were performed under non-lytic conditions, i.e., with $[P]/[L] = 1/100$. Thus, the experiment permitted the visualization of peptide movements on vesicle membranes at different times without membrane rupture. The positioning of each peptide at different times of incubation is schematized in Fig. 3; the interpretation of these schemes suggests that each model proposed at a different time of incubation represents a snapshot of a time course experiment (60 min) initiated by the addition of the peptides to water and in the presence of the vesicles; under this condition, the peptides were randomly coiled (as demonstrated in Table 2). After a short time, the peptide interacts with the lipid membrane in a position more-or-less parallel to the LUV surfaces. The positioning of the amide bonds protected from H/D exchange in the core of the membrane indicates that one or more peptide populations were partially adsorbed to the vesicles. These populations are characterized by different types and numbers of contacts with the membranes and are not "frozen"; throughout the incubation time; these populations of peptides change their positioning in relation to the membrane to achieve more energetically favorable conformations. Thus, the peptide molecules may eventually diffuse on the membrane surface during the course of the experiment. Careful observation of the peptide–membrane interaction models proposed in Fig. 3 reveals the unusual insertion of charged side-chains of Lys residues into the hydrophobic core of the membrane, which causes membrane destabilization, contributing to the occurrence of frequent conformational changes in the peptide chain. Thus, considering that the N-termini of all peptides remain positioned outside the membrane during most of the incubation time course, the frequent conformational changes in the remaining regions of the peptide chain would contribute to the bilayer destabilization. Under the conditions described above, some regions of the membranes reaches a critical concentration of peptides, followed by the consequent leakage of vesicles. The results above support the hypothesis that the interaction of the synthetic mastoparan peptides (MK analogs) with PC and PCPG membranes occurs basically through the carpet model. Therefore, the peptide adsorbs on the membrane surface, forming partially helical structures, which insert some parts of the α-carbon backbone into the core of the membrane, changing the conformation constantly but always maintaining its positioning roughly parallel to the external surface of the membrane. The positioning of the α-carbon partially embedded into the membrane core with frequently changing conformations must cause membrane destabilization and leakage of the vesicle contents. Considering the number of amino acid residues embedded into the membrane core as a criteria for evaluating peptide–membrane interaction, peptides MK7, MK89, MK4589, and MK58911 present the highest numbers of contacts with the core of the anionic (PC) membranes and therefore are expected to present the highest hemolytic activity amongst the mastoparan MK analogs. Meanwhile, the peptides MK4589, MK4578911, and MK45789 interact more strongly with the zwitterionic (PCPG) membranes (Fig. 3A and B) and therefore are expected to present the highest antibiotic activity.

Structure–activity relationship for the MK analog peptides

This study focuses on the structure–activity relationship of mastoparan-like peptides by varying the number and positioning of Lys residues along the peptide chain. Nevertheless, this variation also causes simultaneous changes in the mean hydrophobicity of the peptides as well as in other structural parameters, such as the hydrophobic moment, the size of the polar face and the overall amphipathicity.

It is important to emphasize that the mast cell degranulation activity is directly dependent on the interaction of the peptides with a membrane coupled G-protein receptor; this interaction requires a perfect fit of the secondary structure of the peptide with its binding site to the G_α sub-unit of the G-protein [17,28]. As peptides MK9 and MK89 were the most active analogs in relation to mast cell degranulation, it seems that the positioning of Lys residues at positions 8 and/or 9 is important for the correct binding of the peptides (ligands) to the binding site at the G_α sub-unit.

The hemolytic activity seems to be directly dependent on the membrane perturbation caused by the peptides due to their interaction with the zwitterionic membrane of the erythrocytes. The most active hemolytic peptides assayed were the analogs MK9, MK89, MK58911, and MK5. These peptides present from one to four Lys residues, with hydrophobicity values changing from 0.126 to −0.067 and hydrophobic moments changing from 0.163 to 0.243; it is difficult to correlate these variables with the hemolytic potency of the peptides, as they are distributed in a large range of values. If the total number of amino acid residues of each peptide

embedded into the membrane core (as seen in Fig. 3) is considered to explain the intensity of membrane perturbation, it would be easy to explain the activities of peptides MK9, MK89, and MK58911, but this argument would not justify why peptide MK5 is so active and why MK4589 is poorly hemolytic. However, if the number of amino acid residues from the C-terminal region of each peptide that are continuously embedded into the membrane of PC vesicles (Fig. 3A) is used as a criterion to evaluate the extent of membrane perturbation of the zwitterionic membranes, there is a strongly correlation with the intensity of hemolysis. Peptides MK9, MK89, MK58911, and MK5 present the highest number of amino acid residues in the C-terminal regions of their respective molecules continuously embedded into the membrane core, amongst all the MK analogs.

If the apparent extent of the hydrophilic or hydrophobic surface of each peptide shown in Fig. 6 is used as a criterion to explain the hemolytic potency of the MK analog peptides, no correlations are observed, because the most active peptides include molecules presenting large hydrophilic surfaces (MK578) as well as peptides with reduced hydrophilic surfaces (MK5, and MK9).

The assays of antibiosis revealed that the peptides MK4589, MK45789, and MK4578911 presented a wide spectrum of activity, with very potent action against both Gram-positive and Gram-negative bacteria, being more active even than chloramphenicol. A general physicochemical feature of these peptides is that they presented from four to six lysine residues in their sequences, with five to seven net positive charges, mean hydrophobicity values from −0.087 to −0.280, and hydrophobic moments ranging from 0.072 to 0.248. A careful observation of the schemes of peptide–membrane interaction with the anionic PCPG vesicles (which mimic bacterial cells) shown in Fig. 3B reveals that these peptides have the highest number of amino acid residues embedded into the membrane core (from eight to nine), suggesting that they must interact more strongly with the bacterial membrane than the remaining MK analogs.

Amongst the mastoparans of the MK series, the analogs presenting the most potent antibiotic activities have the largest apparent hydrophilic surfaces, i.e., the highest numbers of Lys residues. This correspondence is most likely related to the neutralization of the anionic character of the PCPG vesicles by the highly cationic characteristics of the MK4589, MK45789, and MK4578911 analogs, favoring the deeper interaction of these peptides with the bacterial membranes compared to the analogs with fewer Lys residues in their sequences. The MIC values of these peptides against Gram-negative and Gram-positive bacteria are approximately 16 μg/mL, while the value for mastoparan-AF is 130 μg/mL [23], and for the peptide anoplin the value ranges from 25 to 50 μg/mL [21]. Therefore, the antimicrobial activity of the peptides MK4589, MK45789, and MK4578911 is very high compared to other peptides that are considered to be highly active.

Conclusion

The initial rationale for engineering mastoparan analog peptides was based on the replacement of certain hydrophobic residues in the hydrophilic face of the peptide molecules by Lys residues. The effects of two different residue replacement strategies were investigated: (i) the individual replacement of Lys residues by Ala, one by one, in a type of Ala scan; and (ii) the replacement of Leu or Ala residues by Lys, in a type of Lys scan. These strategies resulted in a series of peptides presenting net positive charges from +1 to +7, different values of mean hydrophobicity per residue, and different hydrophobic moments. Thus, 10 synthetic mastoparans, tetradecapeptides amidated at their C-termini, were assayed for some typical biological activities for this group of peptides: mast cell degranulation, hemolysis, and antibiosis.

Considering that the mast cell degranulation depends on the ligand (peptide)-receptor (G_α sub-unit of a G-protein), the apparent structural requirement for optimizing this activity was the existence of one or two Lys residues at positions 8 and/or 9. It was difficult to establish a relationship between this activity and the biophysical parameters, namely the mean hydrophobicity per residue and hydrophobic moments.

Regarding hemolysis, one structural aspect that that seems to be strongly correlated with the potency of this activity is the number of amino acid residues from the C-terminus of each peptide that are continuously embedded into the zwitterionic membrane of erythrocytes, probably due to the contribution of this structural feature to the membrane perturbation.

The antibiotic activity of the engineered mastoparan MK analogs seems to be directly dependent on the apparent extension of their hydrophilic surface, i.e., their molecules must have from four to six Lys residues between positions 4 and 11 of the peptide chain to achieve activities comparable to or higher than the reference antibiotic compounds.

Therefore, to optimize the antibacterial activity of mastoparans, it is important have Lys residues at positions 4, 5, 7, 8, 9, and 11 of the tetradecapeptide chain, with the other positions occupied by hydrophobic residues, and with the C-terminal residue in the amidated form. These criteria resulted in highly active AMPs, with highly reduced (or no) hemolytic and mast cell degranulating activities.

Conflict of interest statement

The authors declare no conflict interest.

A few words about Abba Kastin

The recognition of Abba Kastin on the occasion of his retirement as Editor-in-chief of PEPTIDES is an auspicious occasion in the academic history of peptide research abroad. During 35 years Abba fought to provide an internationally recognized vehicle to disseminate scientific results about the structure and activity of all types of biologically active peptides. The permanently open mind of Abba Kastin made him always ready to accept new challenges in peptide research, expanding the borders of the “peptidology”, paving the way for all of us to have access to a high level generalist peptide journal. The books he edited/wrote, especially the well-known editions of “Handbook of Biologically Active Peptides” have tremendous importance and became very popular in peptide science because they presented updated information in a wide range of topics, in a style eminently readable. Ten years serving as member of the Editorial Board gave me pleasant opportunities to discuss, and to share many different scientific and technical aspects of the editorial board with him. During this time I learned to appreciate some aspects of his personality, such as the talent to identify and honor the merits and the skills of the colleagues. With his very enthusiastic way Abba attracted us to publish the results of our research about insect venom toxins in PEPTIDES, which in turn attracted many other toxinologists abroad to do the same. Abba: every time you came to Brazil for lectures, you created a legion of admirers in our scientific community due to your extraordinary goodwill, attention and creativity to deal with the audience. Thank you by the friendship, by the respect that you always expressed, and by the many lessons you gave us.

Mario S. Palma

Acknowledgments

This research is supported by grants from FAPESP (BIOprospecTA Proc. 2011/51684-1), CNPq and Instituto Nacional de Ciência e Tecnologia de Investigação em Imunologia-iii (INCT/CNPq-MCT). MSP and JRN are researchers for the Brazilian Council for Scientific and Technological Development (CNPq).

Appendix A. Supplementary data

Supplementary data associated with this article can be found, in the online version, at http://dx.doi.org/10.1016/j.peptides.2015.04.021

References

[1] Argiolas A, Pisano JJ. Facilitation of phospholipase A_2 activity by mastoparans, a new class of mast cell degranulating peptides from wasp venom. J Biol Chem 1983;258:13697–702.
[2] Argiolas A, Pisano JJ. Isolation and characterization of two new peptides, mastoparan C and crabrolin, from venom of the european hornet, *Vespa crabro*. J Biol Chem 1984;259:10106–11.
[3] Blondelle SE, Forood B, Houghten RA, Perez-Paya E. Secondary structure induction in aqueous vs membrane-like environments. Biopolymers 1997;42:489–98.
[4] De Souza BM, da Silva AV, Resende VM, Arcuri HA, Dos Santos Cabrera MP, Ruggiero Neto J, et al. Characterization of two novel polyfunctional mastoparan peptides from the venom of the social wasp *Polybia paulista*. Peptides 2009;30:1387–95.
[5] De Souza BM, Palma MS. Monitoring the positioning of short polycationic peptides in model lipid bilayers by combining hydrogen/deuterium exchange and electrospray ionization mass spectrometry. Biochim Biophys Acta Biomembr 2008;1778:2797–805.
[6] De Souza BM, Dos Santos Cabrera MP, Ruggiero-Neto J, Palma MS. Investigating the effect of different positioning of lysine residues along the peptide chain of mastoparans for their secondary structures and biological activities. Amino Acids 2011;40:77–90.
[7] Dos Santos Cabrera MP, De Souza BM, Fontana R, Konno K, Palma MS, de Azevedo Jr WF, et al. Conformation and lytic activity of eumenine mastoparan: a new antimicrobial peptide from wasp venom. J Pept Res 2004;64:95–103.
[8] Dos Santos Cabrera MP, Costa ST, De Souza BM, Palma MS, Ruggiero JR, Ruggiero-Neto J. Selectivity in the mechanism of action of antimicrobial mastoparan peptide Polybia-MP1. Eur Biophys J 2008;37:879–91.
[9] Dos Santos Cabrera MP, Arcisio-Miranda M, da Costa LC, De Souza BM, Broggio-Costa ST, Palma MS, et al. Interactions of mast cell degranulating peptides with model membranes: a comparative biophysical study. Arch Biochem Biophys 2009;486:1–11.
[10] Dos Santos Cabrera MP, Alvares DS, Leite NB, De Souza BM, Palma MS, Riske KA, et al. New insight into the mechanism of action of wasp mastoparan peptides: lytic activity and clustering observed with giant vesicles. Langmuir 2011;27:10805–13.
[11] Dos Santos Cabrera MP, Arcisio-Miranda M, Gorjao R, Leite NB, De Souza BM, Curi R, et al. Influence of the bilayer composition on the binding and membrane disrupting effect of Polybia-MP1, an antimicrobial mastoparan peptide with leukemic T-lymphocyte cell selectivity. Biochemistry 2012;51:4898–908.
[12] Eisenberg D, Schwarz E, Komaromy M, Wall R. Analysis of membrane and surface protein sequences with the hydrophobic moment plot. J Mol Biol 1984;179:125–42.
[13] Gallo RL, Huttner KM. Antimicrobial peptides: an emerging concept in cutaneous biology. J Investig Dermatol 1998;111:739–43.
[14] Hancock REW, Chapple DS. Peptide antibiotics. Antimicrob Agents Chemother 1999;43:1317–23.
[15] Henriksen JR, Andresen TL. Thermodynamic profiling of peptide membrane interactions by isothermal titration calorimetry: a search for pores and micelles. Biophys J 2011;101:100–9.
[16] Higashijima T, Wakamatsu K, Takemitsu M, Fujino M, Nakajima T, Miyazawa T. Conformational change of mastoparan from wasp venom on binding with phospholipid membrane. FEBS Lett 1983;152:227–30.
[17] Higashijima T, Uzu S, Nakajima T, Ross EM. Mastoparan, a peptide toxin from wasp venom, mimics receptors by activating GTP-binding regulatory proteins (G proteins). J Biol Chem 1988;263:6491–4.
[18] Hilpert K, Volkmer-Engert R, Walter T, Hancock RE. High-throughput generation of small antibacterial peptides with improved activity. Nat Biotechnol 2005;23:1008–12.
[19] Kim YS, Cha HJ. Disperse distribution of cationic amino acids on hydrophilic surface of helical wheel enhances antimicrobial peptide activity. Biotechnol Bioeng 2010;107:216–23.
[20] Konno T, Meguro H, Tuzimura K. D-Pantolactone as a circular dichromism (CD) calibration. Anal Biochem 1975;67:226–32.
[21] Konno K, Hisada M, Naoki N, Itagaki Y, Nakata Y, Miwa A, et al. Anoplin, a novel antimicrobial peptide from the venom of solitary wasp *Anoplius samariensis*. Biochem Biophys Acta 2001;1550:70–80.
[22] Leite NB, da Costa LC, Dos Santos Alvares D, Dos Santos Cabrera MP, De Souza BM, Palma MS, et al. The effect of acidic residues and amphipathicity on the lytic activities of mastoparan peptides studied by fluorescence and CD spectroscopy. Amino Acids 2011;40:91–100.
[23] Lin CH, Hou RF, Shyu CL, Shia WY, Lin CF, Tu WC. In vitro activity of mastoparan-AF alone and in combination with clinically used antibiotics against multiple-antibiotic-resistant *Escherichia coli* isolates from animals. Peptides 2012;36:114–20.
[24] Luo P, Baldwin RL. Mechanism of helix induction by trifluoroethanol: a framework for extrapolating the helix-forming properties of peptides from trifluoroethanol/water mixtures back to water. Biochemistry 1997;36:8413–21.
[25] Meletiadis J, Meis JGM, Mouton JW, Donnelly JP, Verweij PE. Comparison of NCCLS and 3-(4,5-dimethyl-2-thiazyl)-2,5-diphenyl-2*H*-tetrazolium bromide (MTT) methods of in vitro susceptibility testing of filamentous fungi and development of a new simplified method. J Clin Microbiol 2000;38:2949–54.
[26] Mendes MA, Souza BM, Santos LD, Palma MS. Structural characterization of novel chemotactic and mastoparan peptides from the venom of the social wasp *Agelaia pallipes pallipes* by high performance liquid chromatography/electrospray ionization tandem mass spectrometry. Rapid Commun Mass Spectrom 2004;18:636–42.
[27] Mendes MA, De Souza BM, Marques MR, Palma MS. Structural and biological characterization of two novel peptides from the venom of the neotropical social wasp *Agelaia pallipes pallipes*. Toxicon 2004;44:67–74.
[28] Mendes MA, Palma MS. Two new bradykinin-related peptides from the venom of the social wasp *Protopolybia exigua* (Saussure). Peptides 2006;27:2632–9.
[29] Okano Y, Takagi H, Tohmatsu T, Nakashima S, Kuroda Y, Saito K, et al. A wasp venom mastoparan-induced polyphosphoinositide breakdown in rat peritoneal mast cells. FEBS Lett 1985;188:363–6.
[30] Palma MS. Peptides as toxins/defensins. Amino Acids 2011;40:1–4.
[31] Rohl CA, Baldwin RL. Deciphering rules of helix stability in peptides. Methods Enzymol 1998;295:1–26.
[32] Santos LD, Pinto JRAS, Menegasso ARS, Saidemberg DM, Garcia AMC, Palma MS. Proteomic profiling of the molecular targets of interactions of the mastoparan peptide Protopolybia MP-III at the level of endosomal membranes from rat mast cells. Proteomics 2012;12:2682–93.
[33] Sforça ML, Oyama Jr S, Canduri F, Lorenzi CCB, Pertinhez TA, Konno K, et al. How C-terminal carboxyamidation alters the biological activity of peptides from the venom of the Eumenine solitary wasp. Biochemistry 2004;43:5608–17.
[34] Silva AVR, De Souza BM, dos Santos Cabrera MP, Dias NB, Gomes PC, Ruggiero Neto J, et al. The effects of the C-terminal amidation of mastoparans on their biological actions and interactions with membrane-mimetic systems. Biochim Biophys Acta 2014;1838:2357–68.
[35] Solomon KR, Kurt-Jones EA, Saladino RA, Stack AM, Dunn IF, Ferretti M, et al. Heterotrimeric G proteins physically associated with the lipopolysaccharide receptor CD14 modulate both in vivo and in vitro responses to lipopolysaccharide. J Clin Invest 1998;102:2019–27.
[36] Wang KR, Zhang BZ, Zhang W, Yan JX, Li J, Wang R. Antitumor effects, cell selectivity and structure–activity relationship of a novel antimicrobial peptide Polybia-MPI. Peptides 2008;29:963–8.
[37] Wang KR, Yan JX, Zhang BZ, Song JJ, Jia PF, Wang R. Novel mode of action of Polybia-MPI, a novel antimicrobial peptide, in multi-drug resistant leukemic cells. Cancer Lett 2009;278:65–72.
[38] Won HS, Kang SJ, Choi WS, Lee BJ. Activity optimization of an undecapeptide analogue derived from a frog-skin antimicrobial peptide. Mol Cells 2011;31:49–54.
[39] Xu X, Li J, Lu Q, Yang H, Zhang Y, Lai R. Two families of antimicrobial peptides from wasp (*Vespa magnifica*) venom. Toxicon 2006;47:249–53.
[40] Xu X, Yang H, Yu H, Li J, Lai R. The mastoparanogen from wasp. Peptides 2006;27:3053–7.
[41] Yandek LE, Pokorny A, Almeida PF. Wasp mastoparans follow the same mechanism as the cell-penetrating peptide transportan 10. Biochemistry 2009;48:7342–51.
[42] Zasloff M. Antimicrobial peptides of multicellular organisms. Nature 2002;415:389–95.